TRANSFORMATION BETWEEN COMPLEX SCATTERING LENGTH AND BINDING ENERGY* **

Q. Haider

Department of Physics and Engineering Physics, Fordham University
Bronx, NY 10458, USA

Lon-Chang Liu

Theoretical Division, Los Alamos National Laboratory
Los Alamos, NM 87545, USA

(Received January 7, 2014)

The use of scattering length of particle–target interaction due to real-valued potential to study the bound states of the particle–target system is well known in nuclear and atomic physics. In view of the current interest in using η-nucleus scattering length to infer the existence of η-mesic nucleus, we derive general analytic expressions that relate the binding energy and half-width of an unstable bound state to the complex-valued scattering length due to the same particle-target interaction.

DOI:10.5506/APhysPolB.45.827
PACS numbers: 24.60.Dr, 13.75.Gx, 21.10.Dr

1. Introduction

The existence of eta-mesic nucleus, a novel nucleus with an excitation energy of about 540 MeV, first predicted more than 25 years ago [1], has led to several theoretical studies [2, 3] aimed at understanding the underlying interaction between an eta (η) meson and a nucleus. While there is difference of opinion on the size of the nucleus in which the η can be bound, there is general agreement that theoretical calculations, irrespective of the formalism and ηN interaction model used, provide compelling reason to believe that η-mesic nucleus does indeed exist with nuclear mass number greater than 10 [2].

---

* Presented at the II International Symposium on Mesic Nuclei, Kraków, Poland, September 22–25, 2013.

** All correspondences should be sent to haider@fordham.edu

Since 1986, the search for η-mesic nucleus has been conducted at various laboratories in the USA, Europe and Japan. The most promising indication of the existence of η-mesic nucleus comes from an experiment performed at COSY-GEM (Jülich) [4] using the $(p,{}^3\mathrm{He})$ reaction on $^{27}\mathrm{Al}$. This experimental result has, in turn, further encouraged efforts in searching the possibility of forming η-mesic nucleus in light nuclei such as $^{3,4}\mathrm{He}$ [3–5], as advocated by some researchers. Clearly, this latter possibility is directly related to the magnitude of the η-nucleus scattering length a.

In a recent work, Niskanen and Machner [6] explored the relation between the binding energy and width of an η-mesic nucleus and the complex-valued η-nucleus scattering length. One of the underlying ideas of such study is that an experimental determination of a via final-state interaction between η and a nucleus would indicate the existence or nonexistence of an η-nucleus s-wave bound state. Independent of the way how the scattering length or the binding energy is modeled or measured, we will see that the functional relation between these two observables is, in fact, model-independent. Hence, this dependence is an interesting subject on its own. In this paper, we present the model-independent features of this functional dependence.

2. Polar representation of observables

The s-wave scattering amplitude is given by

$$f = \frac{e^{2i\delta} - 1}{2ik} = \frac{1}{k\cot\delta - ik}\,, \tag{1}$$

where δ is the phase shift which is complex-valued when an optical potential is used in calculating it and k is the final-state channel momentum. For exponentially bound potentials,

$$k\cot\delta = \frac{1}{a} + \frac{1}{2}rk^2 + \dots\,, \tag{2}$$

where a is the scattering length and r is the effective range. In the limit $k \to 0$, the first term dominates, *i.e.*,

$$k\cot\delta = \frac{1}{a}\,, \tag{3}$$

and

$$f = \frac{1}{1/a - ik}\,. \tag{4}$$

The bound-state pole occurs at $k_{\mathrm{pol}} = -i/a$ which leads to

$$k_{\mathrm{pol}}^2 = -\frac{1}{a^2}\,. \tag{5}$$

It is useful to use the polar representation in the complex a plane so that

$$a = |a| \exp(i\gamma) \equiv x + iy \,, \tag{6}$$

with

$$x = \mathrm{Re}[a] = |a| \cos\gamma \,, \qquad y = \mathrm{Im}[a] = |a| \sin\gamma \,, \qquad \gamma = \arctan\left(\frac{y}{x}\right) \,. \tag{7}$$

It follows that

$$k_{\mathrm{pol}}^2 = -\frac{1}{|a|^2} \, \exp(-2i\gamma) \,. \tag{8}$$

The complex energy B is, therefore, given by

$$B = \frac{k_{\mathrm{pol}}^2}{2\mu} = -|B| \, \exp(-2i\gamma) \,, \tag{9}$$

where μ is the reduced mass of the bound particle and

$$|B| = \frac{1}{2\mu|a|^2} \,. \tag{10}$$

In the Cartesian representation,

$$B \equiv E - i\frac{\Gamma}{2} \equiv u + iv \,, \tag{11}$$

where E and $\Gamma/2$ denote, respectively, the binding energy and half-width of the bound state. It follows from Eqs. (6) and (7) that

$$u \;\equiv\; E = -\frac{x^2 - y^2}{2\mu|a|^4} \,, \tag{12}$$

$$v \;\equiv\; -\frac{\Gamma}{2} \;=\; \frac{2xy}{2\mu|a|^4} \,. \tag{13}$$

The polar representation in the a-plane, equation (6), was used by Balakrishnan *et al.* [7] to calculate the energies and widths of bound states as functions of complex scattering lengths in multi-channel atom-molecule collisions. In Section 3 we expand the polar representation to include the k_{pol}- and B-planes, and determine the respective physical domains. Using these domains, we solve in Section 4 the inverse problem, namely, finding the value of complex a for a given value of complex energy B.

3. Physical domains on the complex planes

If we denote

$$k_{\rm pol} = R + iI\,, \tag{14}$$

then

$$k^2_{\rm pol} = R^2 - I^2 + 2iRI\,. \tag{15}$$

Hence, we obtain from Eqs. (9) and (11)

$$2\mu E = R^2 - I^2 = -\frac{1}{|a|^2}\cos 2\gamma\,, \tag{16}$$

$$2\mu\left(\frac{\Gamma}{2}\right) = -2RI = -\frac{1}{|a|^2}\sin 2\gamma\,. \tag{17}$$

Because $E < 0$ (the bound state) and $\Gamma > 0$ (by definition), Eqs. (16) and (17) are, respectively, equivalent to

$$\left(R^2 - I^2\right) < 0 \quad \text{and} \quad RI < 0\,. \tag{18}$$

The first inequality requires $|R| < |I|$. Since a bound state has $I > 0$ (*i.e.* a decaying outgoing wave), the second inequality then requires $R < 0$. In summary, the requirements $|R| < |I|$, $I > 0$ and $R < 0$ indicate that the bound-state (in the literature it is also called quasi-bound state) poles are situated in the second quadrant (but above the diagonal line) of the complex $k_{\rm pol}$-plane.

Equations (16) and (17) further indicate that $E < 0$ and $\Gamma > 0$ require, respectively, that $\cos 2\gamma > 0$ and $\sin 2\gamma < 0$. This, in turn, requires $3\pi/2 < 2\gamma < 2\pi$ or $3\pi/4 < \gamma < \pi$. The complex scattering length, a, is therefore situated in the second quadrant but below the diagonal line in the complex a-plane. In other words, on the a-plane the scattering length satisfies simultaneously

$$\mathrm{Im}[a] > 0\,, \qquad \mathrm{Re}[a] < 0\,, \qquad |\mathrm{Im}[a]| < |\mathrm{Re}[a]|\,. \tag{19}$$

The third inequality was also shown in Ref. [2]. The physical domains in the a-, $k_{\rm pol}$-, and B-planes are shown in Figs. 1–3, respectively. When the polar angle, γ, in the a-plane turns counter clockwise, the corresponding polar angles in the $k_{\rm pol}$- and B-planes turns in the opposite direction (see Section 5.1).

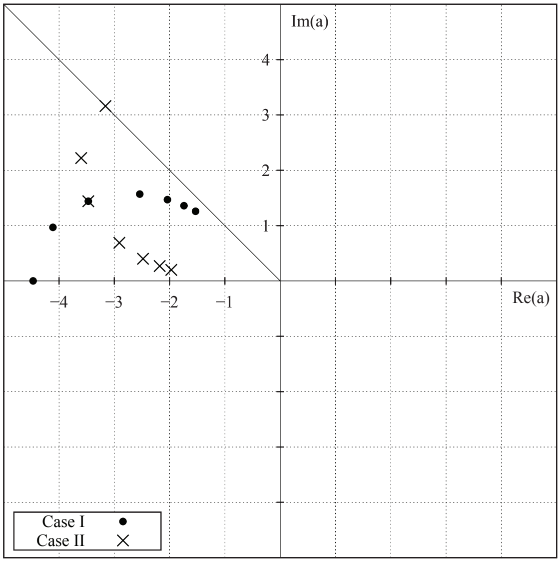

Fig. 1. The complex scattering length plane. The physical domain is the entire lower triangular region of the 2nd quadrant. The meaning of the solid circles and the crosses are given in the text.

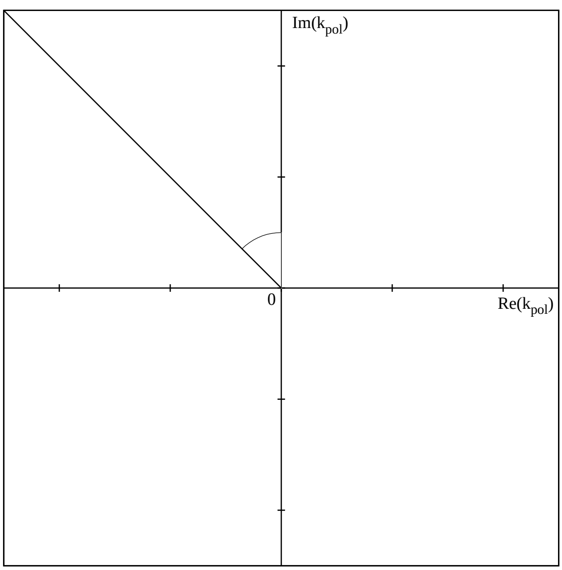

Fig. 2. The complex momentum plane. The physical domain is the entire upper triangular region of the 2nd quadrant. The arc near the origin indicates the corresponding polar-angle range.

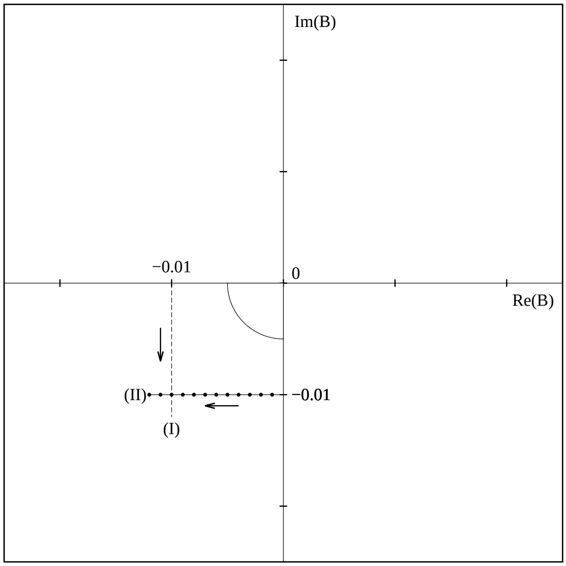

Fig. 3. The binding-energy plane. The physical domain is the entire 3rd quadrant. The arc indicates the polar-angle range. The trajectories shown by the downward dashed line and the horizontal linked-dotted line are explained in the text.

4. Inverse mapping

From Eqs. (10), (12), and (13), we get

$$u = -2\mu|B|^2\left(x^2 - y^2\right) \tag{20}$$

and

$$v = 2\mu|B|^2(2xy)\,. \tag{21}$$

The inverse mapping is obtained by solving the above coupled equations and the result is

$$x = \left(-\frac{1}{2|B|\sqrt{\mu}}\right)\sqrt{-u + \sqrt{u^2 + v^2}}\,, \tag{22}$$

$$y = \left(\frac{1}{2|B|\sqrt{\mu}}\right)\sqrt{u + \sqrt{u^2 + v^2}}\,. \tag{23}$$

In choosing the branch of the square roots, the properties associated with the physical domains discussed in Section 3 have been used. For bound states, $u < 0$. Hence, $u = -|u|$ in the last two equations.

5. Results and discussion

5.1. Application of the inverse mapping

As examples of the application of the inverse mapping, we have considered two cases. The departing trajectories on the B-plane are shown in Fig. 3. Case I corresponds to fixing E but varying $\Gamma/2$ in the direction given by the downward arrow along the dashed line. Case II corresponds to fixing the value of $\Gamma/2$, while varying E along the horizontal linked-dotted line in the direction shown by the leftward arrow. The resulting a (calculated with $2\mu = 5\ \mathrm{fm}^{-1}$) are shown, respectively, as the left-to-right solid circles and the descending crosses in Fig. 1. One notes that the polar angles, γ, of the successive left-to-right solid circles in Fig. 1 turn clockwise, while those of the original B-points along the downward dashed line in Fig. 3 turn counter clockwise. This reversal of the sense of the turning is a consequence of the opposite signs in front of the polar angles in Eqs. (6) and (9).

5.2. Role of nuclear mass in the binding of η

From Eqs. (22) and (23), one notes that the magnitudes of the real and imaginary parts of the scattering length a are inversely proportional to $\sqrt{\mu}$. For η-mesic nucleus, μ is the reduced mass of η, which increases as nuclear mass increases. This, in turn, indicates that for η to have a given binding energy $|E|$ in a lighter nucleus, it requires a larger $|\mathrm{Re}[a]|$ than that for η to have the same binding energy $|E|$ in heavier nuclei. This is why the ηN model of Ref. [1] does not predict the existence of ${}^{3,4}\mathrm{He}_\eta$, while models giving larger $|a_{\eta N}|$ (and, hence, larger $|a_{\eta A}|$) do predict these light η-mesic nuclei.

5.3. Remark on the sign convention of the scattering length

The scattering length approximation is often written as

$$k \cot \delta = -\frac{1}{a}\,. \tag{24}$$

To avoid confusion, let us denote $-a = \mathcal{A}$ in Eq. (24). The polar representation of a, Eq. (6), then leads to the following equations

$$\mathcal{A} = -|a|e^{i\gamma} = |a|e^{i(\pi+\gamma)} = |a|e^{i\theta}\,, \tag{25}$$

where we have defined $\theta = \pi + \gamma$. By repeating the algebra leading Eq. (3) to Eq. (19), we have noted that the forms of Eqs. (8), (9), (16), (17) remain unchanged, except that in these equations the variable 2γ will be replaced by 2θ. However, this variable change has no consequence on the final results because $\cos 2\theta = \cos 2\gamma$ and $\sin 2\theta = \sin 2\gamma$. In other words, when one goes from (Re$[a]$, Im$[a]$) to determine $(E, \Gamma/2)$, the result is independent of the sign of the scattering length, a. This is because $k^2_{\rm pol}$ is independent of the sign of a. However, because $-a = \mathcal{A}$, the physical domain on the $\mathcal{A}$-plane will be the upper triangular region of the 4$^{\rm th}$ quadrant. If we define $\mathcal{A} = x' + iy'$, then $x' = -x$ and $y' = -y$, with the x and y given, respectively, by Eqs. (22) and (23). However, we will still have the inequality $|{\rm Im}[\mathcal{A}]| < |{\rm Re}[\mathcal{A}]|$, the same as the third inequality in Eq. (19).

6. Summary

We have studied the complex mappings $a \to B$ and $B \to a$. By using the physics implied by the momentum of a bound state, we have determined the physical domain of a (Fig. 1). The a satisfies the properties given in Eq. (19).

Our analytic expressions (Eqs. (22) and (23)) are interaction-model independent so long as the potential of the particle-target interaction belongs to the class of exponentially bound potentials so that the low-energy expansion, Eq. (2), can be made. The only kinematic approximation used in our derivation is $k^2_{\rm pol}/2\mu \simeq \sqrt{k^2_{\rm pol} + \mu^2} - \mu$ which is a very good approximation for binding energies. We emphasize that the model dependence of the interaction dynamics does come into play when one theoretically calculates the scattering length, a, and the binding energies, B. However, once one of these two observables is calculated (or measured), then the remaining one is determined by Eqs. (16) and (17) or, *vice versa*, by Eqs. (22) and (23). These analytic expressions offer, therefore, a means of making consistency test of interaction models or measurements. We mention, among others, that these analytical expressions can be calculated readily by means of hand calculators. Finally, they can be used to gain insight into the trend of bound-state formation as elucidated by the example discussed in Section 5.2.

We would like to thank Ariel Fragale, a senior physics major at Fordham University for her assistance with the figures. One of us (Q.H.) would like to thank Professor Paweł Moskal of the Jagiellonian University for the hospitality extended to him during his stay at Kraków.

REFERENCES

[1] Q. Haider, L.C. Liu, *Phys. Lett.* **B172**, 257 (1986).

[2] Q. Haider, L.C. Liu, *Phys. Rev.* **C66**, 045208 (2002) and references therein.

[3] N.G. Kelkar, K.P. Khemchandani, N.J. Upadhyay, B.K. Jain, *Rep. Prog. Phys.* **76**, 066301 (2013) and references therein.

[4] A. Budzanowski *et al.*, *Phys. Rev.* **C79**, 012201(R) (2009).

[5] V. Krzmien, P. Moskal, J. Smyrski, *Acta Phys. Pol. B Proc. Suppl.* **2**, 141 (2009) .

[6] J.A. Niskanen, H. Machner, *Nucl. Phys.* **A902**, 40 (2013).

[7] N. Balakrishnan, V. Kharchenko, R.C. Forrey, A. Delgarno, *Chem. Phys. Lett.* **280**, 5 (1997).